INRIA

INSTITUT NATIONAL DE RECHERCHE EN INFORMATIQUE ET EN AUTOMATIQUE

Ground resonance monitoring for hinged-blades helicopters: statistical CUSUM approach

Ahmed Jhinaoui — Laurent Mevel — Joseph Morlier — Leonardo Sanches

N° 7431

Octobre 2010

Stochastic Methods and Models

ISSN 0249-6399 ISRN INRIA/RR--7431--FR+ENG

INSTITUT NATIONAL
DE RECHERCHE
EN INFORMATIQUE
ET EN AUTOMATIQUE

INRIA

centre de recherche
RENNES - BRETAGNE ATLANTIQUE

Ground resonance monitoring for hinged-blades helicopters: statistical CUSUM approach

Ahmed Jhinaoui*, Laurent Mevel†, Joseph Morlier‡ , Leonardo Sanches§

Theme : Stochastic Methods and Models
Applied Mathematics, Computation and Simulation
Équipe I4S

Rapport de recherche n° 7431 — Octobre 2010 — 15 pages

Abstract: Works on the problem of helicopter ground resonance and the prediction of related instability zones relay generally on off-line modal analysis, neglecting thus the problem of model's uncertainties. In this paper, an on-line algorithm of detection, built on the CUSUM test, is proposed. A numerical application to simulation data is then reported. The mechanical model developed by [17] is used for simulation and is extended to the class of helicopters with damped structures.

Key-words: helicopter, ground resonance, vibration monitoring, damping coefficient, CUSUM test

This work was supported by the European project FP7-NMP CPIP 213968-2 IRIS.

* INRIA, Centre Rennes - Bretagne Atlantique
† INRIA, Centre Rennes - Bretagne Atlantique
‡ Université de Toulouse, ICA, ISAE/INSA/UPS/ENSTIMAC
§ Université de Toulouse, ICA, ISAE/INSA/UPS/ENSTIMAC

Centre de recherche INRIA Rennes – Bretagne Atlantique
IRISA, Campus universitaire de Beaulieu, 35042 Rennes Cedex
Téléphone : +33 2 99 84 71 00 — Télécopie : +33 2 99 84 71 71

Détection de la résonance au sol pour les hélicoptères á rotors articulés: une approche statistique avec tests CUSUM

Résumé : Les travaux sur le phénomène de résonance au sol des hélicoptères et la prédiction des zones d'instabilité liée utilisent généralement l'analyse modale hors-ligne, négligeant ainsi le problème d'incertitudes sur le modèle. Dans ce rapport, un algorithme de détection en-ligne - utilisant les tests CUSUM- est proposé et des résultats de simulation numérique sont rapportés. Le modèle mécanique développé par [17] est utilisé pour la simulation mais en introduisant des amortissements structurels cette fois-ci.

Mots-clés : hélicoptère, résonance au sol, détection de vibrations, coefficients d'amortissement, test CUSUM

1 Introduction

Ground resonance is an instability that may develop on helicopters when the rotor is spinning on or near the ground, and that may result in the destruction of the structure. Until the 1940's, it was admitted that the phenomenon is due to rotor-blade flutter. But the works lead by Coleman and Feingold [6] between 1942 and 1947 had demonstrated that this instability is self-excited vibrations.

Ground resonance is one of the most dangerous situations a helicopter pilot can face. Inconveniently, this is rather recurring: for instance, the US National Transportation Safety Board reports 41 incidents of ground resonance since 1990. Therefore, several studies have been carried out to analyze, predict and avoid this phenomenon. Among those, one can state the contributions of [7] who focused on understanding and modeling the dynamics of ground and air resonance, [14] who extended the classical theory of Coleman and Feingold -which limits the study to the motions in the plane of the main rotor blades- to include other degrees of freedom, and more recently, [12] who has introduced nonlinear stiffness and damping in the modal analysis of this phenomenon. With the use of numerical methods [18], [8], modeling is going more accurate to locate the zones of instability: a system is unstable when one or more of the damping coefficients drop from positive values to become negative. Unfortunately, aircrafts are a highly time-varying systems depending on many factors and uncertainties so that the off-line modeling is not sufficiently reliable. Thus, the system has to be identified continuously which is very expensive in time and in on-board calculators memory.

The cumulative sum (CUSUM) test, able of on-line monitoring, could be a good alternative that ensures the avoiding of system identification for each flight point with improved confidence and reduced costs. The main idea of this test is to compute a stability criterion at a reference state, and then to track it for any other state. An alarm is triggered when a change is detected on this criterion.

Since its introduction and till the late seventies, works on test theory were dominated by results from statisticians. Then, applications to vibration monitoring have emerged. Recently, some studies have investigated its capacities to detect vibrations such as flutter on aircrafts [13], [19], [3].

The purpose herein is to describe a CUSUM test algorithm for monitoring a drop in damping coefficients, and to apply it to the case of helicopter ground resonance. The paper is organized as follows. Section 2 presents the essential elements of CUSUM test and the building of recursive damping-function residual. Section 3 gives the mechanical model of a helicopter with structural dampers and its equation of motion. Finally, section 4 explains the relevance of choosing the damping coefficients as a criterion of instability, and gives the results of CUSUM test applied to ground resonance case.

2 Generalities on CUSUM test

In this section, we give the main lines of subspace-based residual and CUSUM algorithm.

Let consider the discrete time model, in state space form, of a given system:

$$\left\{ \begin{array}{rcl} X_{k+1} & = & F\ X_k + v_{k+1} \\ Y_k & = & H\ X_k + w_{k+1} \end{array} \right.$$

where $X \in \mathbf{R}^n$ is the state vector, $Y \in \mathbf{R}^r$ the output vector, $F \in \mathbf{R}^{n \times n}$ the transition matrix and $H \in \mathbf{R}^{r \times n}$ the observation matrix. The vectors v and w are noises that are assumed to be white gaussian and zero-mean.

Let $(\lambda_i, \phi_i)_{i=1 \cdots m}$ be the pairs of eigenvalues and eigenvectors given by $det(F - I\lambda_i) = 0$ and $F\phi_i = \lambda_i \phi_i$. These two eigenstructure parameters are stacked into a vector called *modal signature* and defined as: $\theta = \begin{pmatrix} \Lambda \\ vect(\Phi) \end{pmatrix}$ where Λ is the vector of all the eigenvalues λ_i and $\Phi = [H\phi_1 .. H\phi_m]$ is the matrix of observed eigenvectors.

The key feature of system fault detection is to track a change in the modal signature in regard with a given reference modal signature θ_0 [1], [2]. For that, we define a *residual* that will be computed for each new data and that compares between the current signature and the signature at reference. The residual is slightly null near the reference and begins to take greater values when a change is detected.

2.1 Output only-based residual

Given a modal signature at the reference θ_0 (could be found by a subspace-based identification for example), and a set of outputs $(y_k)_{k=1 \cdots N}$ for N samples at a different point θ of covariances $R_i = \mathbf{E}(y_k y_{k-i})$ which can be approximated by $\hat{R}_i = \frac{1}{N} \sum_{k=i+1}^{N} y_k y_{k-i}^T$ for $N \gg 1$, the matrices of observability and of Hankel are:

$$\mathcal{O}_{p+1}(\theta_0) = \begin{bmatrix} \Phi \\ \Phi\Delta \\ \vdots \\ \Phi\Delta^p \end{bmatrix}$$

where $\Delta = diag(\Lambda)$.

$$\mathcal{H}_{p+1,q} = \begin{bmatrix} R_0 & R_1 & \cdots & R_{q-1} \\ R_1 & R_2 & \cdots & R_q \\ \vdots & \vdots & \vdots & \vdots \\ R_p & R_{p+1} & \cdots & R_{p+q-1} \end{bmatrix}$$

$p + q$ is the length of the correlation tail.

Then, an estimate of Hankel matrix is:

$$\hat{\mathcal{H}}_{p+1,q} = Hank(\hat{R}_i) = \frac{1}{N} \sum_{k=1}^{N} \mathcal{Y}_{k,p+1}^{+} \mathcal{Y}_{k,q}^{-,T}$$

where

$$\mathcal{Y}_{k,p+1}^{+} = \begin{pmatrix} y_k \\ \vdots \\ y_{k+p} \end{pmatrix}, \mathcal{Y}_{k,q}^{-} = \begin{pmatrix} y_k \\ \vdots \\ y_{k-q+1} \end{pmatrix}$$

Remark 1 *The matrix of Hankel can be decomposed such that* $\mathcal{H}_{p+1,q} = \mathcal{O}_{p+1}\mathcal{C}_q$, *where* $\mathcal{O}$ *and* $\mathcal{C}$ *are the matrices of observability and controllability. Therefore, a matrix of Hankel corresponds to the reference* θ_0 *if and only if it has the same left kernel as the matrix of observability* $\mathcal{O}_{p+1}(\theta_0)$.

Let S be such kernel. This matrix could be extracted for example by a Single Value Decomposition (SVD) of the matrix of observability. We choose it to be orthogonal, so that: $S^T S = I_s$ and $S^T \mathcal{O}_{p+1}(\theta_0) = 0$. According to Remark 1, when we are near to the reference:

$$S^T(\theta_0)\hat{\mathcal{H}}_{p+1,q} = \frac{1}{N}\sum_{k=1}^{N} S^T(\theta_0)\mathcal{Y}^+_{k,p+1}\mathcal{Y}^{-,T}_{k,q} \simeq 0$$

We build then the residual below, which is widely used in applications dealing with structural vibration monitoring [4]:

$$\begin{aligned}\xi_N(\theta_0) &= \sqrt{N}vec(S^T(\theta_0)\hat{\mathcal{H}}_{p+1,q}) \\ &\simeq \frac{1}{\sqrt{N}}\sum_{k=q}^{N-p} vec(S^T(\theta_0)\mathcal{Y}^+_{k,p+1}\mathcal{Y}^{-,T}_{k,q})\end{aligned}$$

ξ is asymptotically gaussian with a mean null near the reference and different from zero elsewhere. The Jacobian and the covariance matrices of ξ at the reference are:

$$\begin{aligned}\mathcal{J}(\theta_0) &= \lim_{N\to+\infty}\left(-\frac{1}{\sqrt{N}}\frac{\partial}{\partial\theta}\mathbf{E}_{\theta_0}\xi_N(\theta)_{\theta=\theta_0}\right) \\ \Sigma(\theta_0) &= \lim_{N\to+\infty}\mathbf{E}_{\theta_0}\left(\xi_N(\theta_0)\xi_N(\theta_0)^T\right)\end{aligned}$$

2.2 Residual for damping tracking

For complex systems like aircrafts, detecting a change in the modal signature does not mean the failure of the structure. Aircrafts eigenstructure is changing for every new flight point. Only a decrease in damping coefficients can reveal an evolution toward instability. Therefore, the residual must be expressed in term of damping and the problem is then to detect a decrease in a damping coefficient from its reference value ρ_0 to another value ρ. The new residual writes [13]:

$$\xi_N(\rho_0) = \frac{1}{\sqrt{N}}\sum_{k=q}^{N-p}\mathcal{Z}_k$$

Where $\mathcal{Z}_k$, called *recursive residual*, is:

$$\mathcal{Z}_k = \hat{\mathcal{J}}(\rho_0)^T\hat{\Sigma}(\theta_0)^{-1}vec\left(\ S^T(\theta_0)\mathcal{Y}^+_{k,p+1}\mathcal{Y}^{-,T}_{k,q}\ \right)$$

It is this recursive residual which is used for CUSUM test and which gives the detection its on-line character as explained in the next subsection. $\hat{\mathcal{J}}$ and $\hat{\Sigma}$ are estimates of the Jacobian and covariance matrices. $\hat{\mathcal{J}}(\rho_0) = \hat{\mathcal{J}}(\theta_0)\hat{\mathcal{J}}_{\theta\rho|\theta_0\rho_0}$, where $\hat{\mathcal{J}}_{\theta\rho|\theta_0\rho_0}$ is the sensitivity of θ w.r.t. ρ. Consistent estimates of these matrices are proposed in [2] and [5].

2.3 CUSUM test

CUSUM test was introduced first by [15] for change detection in sequential process. The idea is to compute a cumulative sum of recursive residual for each new sample data and to compare it to its maximum in order to detect if a change has occurred. In our case of study, the test writes:

$$\begin{cases} S_k(\rho_0) = \Sigma(\theta_0)^{-1/2} \sum_{j=q}^{k} \mathcal{Z}_j(\rho_0) \\ T_k(\rho_0) = \max_{q \preceq k \preceq N-p} S_k(\rho_0) \\ g_k(\rho_0) = T_k(\rho_0) - S_k(\rho_0) \end{cases}$$

The two hypotheses to test are:

$$\begin{cases} \mathbf{H}_0 : \mathbf{E} g_k(\rho_0) \approx 0 \\ \mathbf{H}_1 : \mathbf{E} g_k(\rho_0) \succ 0 \end{cases}$$

For every sample, S_k and T_k are computed. Hypothesis $\mathbf{H}_1$ is decided when the current sample of damping coefficients ρ_k is under the value of reference ρ_0, namely $S_k - T_k = -g_k(\rho_0) < -\epsilon$ for some threshold ϵ; an alarm is then triggered, as illustrated in Fig. 1.

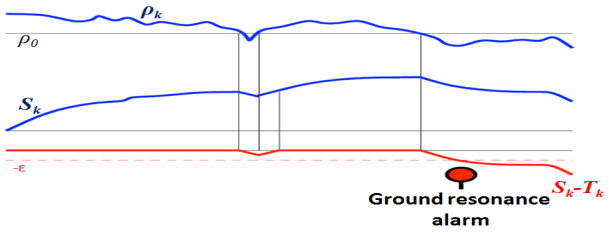

Figure 1: CUSUM test

In order to reject the detection of slight changes, a *minimum magnitude of change* σ is added to the expression of the cumulative sum, such that $S_k(\rho_0) = \Sigma(\theta_0)^{-1/2} \sum_{j=q}^{k} (\mathcal{Z}_j(\rho_0) + \sigma)$.

3 Helicopter model for ground resonance

When the rotor of a helicopter is spinning, angular phase shifts - known as *leading and lagging* angles- can be created on the blades by external disturbances. Basically, this may occur for example when a helicopter with a wheel-type landing gear touches the ground firmly on one corner, and that this shock is transmitted to the blades in form of out of phase angular motions. Those angular motions interact with the elastic parts of the fuselage (the landing gear, mainly) for certain values of rotor's angular velocity. The fuselage starts then to rock laterally. These lateral oscillations amplify the lead-lagging motions which also

Figure 2: Chinook CH-47 Ground resonance test, rear view

amplifies the oscillations, and so on till the divergence and the destruction of the structure when a critical frequency is reached (see Fig. 2).

In this section, we present the dynamical equations of motion that describe this phenomenon, and develop the Linear Time Invariant (LTI) mechanical model in a similar way as described in [17], but adding damping to the structure this time and using the complex notation for simplicity. The class of helicopters considered herein is the one with in-plane hinged blades rotors.

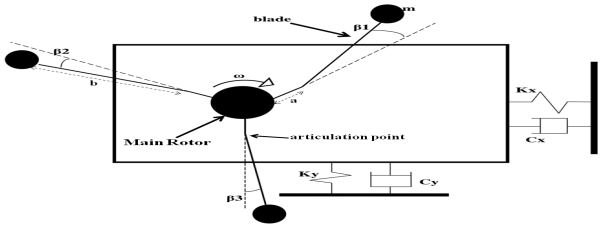

Figure 3: Mechanical model of a helicopter with 3 blades

The fuselage is considered to be a rigid body with mass M, attached to a flexible LG (landing gear) which is modeled by two springs K_x and K_y, and two viscous dampers C_x and C_y as illustrated in Fig. 3. The rotor spinning with a velocity ω, is articulated and the offset between the MR (main rotor) and each articulation is noted a. The blades are modeled by a concentrated mass m at a distance b of the articulation point. A torque stiffness and a viscous damping is present into each articulation.

The case of study is limited to the degrees of freedom below:

- 2 lateral motions of the fuselage in axes x and y
- in-plane angular motion β_k on each blade: with stiffness equal to K_{β_k} and damping C_{β_k}

3.1 Kinetic energy

Let β_k be the k^{th} lead-lag angle, and x and y the two deflections of the fuselage. Using the theorem of Koenig and the complex notation $z = x + iy$. The total kinetic energy of one blade is the sum of the kinetic energy of the circular translation, and that of the rotation about the center of mass of the blade: $T_{p_k} = \frac{1}{2} m \dot{z_k} \bar{\dot{z}_k} + \frac{1}{2} I_z \dot{\beta_k}^2$, where m is the mass of the blade, ω is the angular velocity of the main rotor, I_z the moment of inertia of the k^{th} blade about its

center of mass, and $z_k = x_k + iy_k = z + (a + be^{i\beta_k})e^{i(\omega t+\alpha k)}$ is the coordinate of the k^{th} blade, with $\alpha = \frac{2\pi}{N_b-1}$ and N_b the total number of blades. Then for small displacements β_k, the kinetic energy of one blade writes:

$$\begin{aligned} T_{p_k} &= \frac{1}{2}m(\dot{z}\dot{\bar{z}} + \dot{\bar{z}}ib(\dot{\beta_k} + i\omega\beta_k)e^{i(\omega t+\alpha k)} \\ &+ \dot{z}(-ib)(\dot{\beta_k} - i\omega\beta_k)e^{-i(\omega t+\alpha k)} + b^2\dot{\beta}^2 \\ &- \omega^2 ab\beta^2) + \frac{1}{2}I_z\dot{\beta_k}^2 \end{aligned} \quad (1)$$

Now, if we make the two variable changes below:
$\theta_k = \frac{ib}{N_b}\sum_{j=0}^{N_b-1}\beta_j e^{\frac{2ijk\pi}{N_b}}$ and $\eta_k = \theta_k e^{i\omega t}$, one can demonstrate that:

$$\sum_{k=0}^{N_b-1}\eta_k\bar{\eta}_k = \sum_{k=0}^{N_b-1}\theta_k\bar{\theta}_k = \frac{b^2}{N_b}\sum_{k=0}^{N_b-1}\beta_k^2 \quad (2)$$

and

$$\begin{aligned} \sum_{k=0}^{N_b-1}(\dot{\eta_k} - i\omega\eta_k)(\dot{\bar{\eta}_k} + i\omega\bar{\eta_k}) &= \sum_{k=0}^{N_b-1}\dot{\theta_k}\dot{\bar{\theta}_k} \\ &= \frac{b^2}{N_b}\sum_{k=0}^{N_b-1}\dot{\beta_k}^2 \end{aligned} \quad (3)$$

The kinetic energy of the rotor is the sum of the kinetic energy of each blade. Using (1), (2) and (3), one can write:

$$\begin{aligned} T_{p_r} &= \frac{1}{2}N_b m\dot{z}\dot{\bar{z}} + \frac{1}{2}m[N_b\dot{\bar{z}}\dot{\eta_1} + N_b\dot{z}\dot{\bar{\eta}_1} \\ &+ N_b\sum_{k=0}^{N_b-1}(\dot{\bar{\eta}_k} + i\omega\bar{\eta_k})(\dot{\eta_k} - i\omega\eta_k) \\ &- N_b\omega^2\frac{a}{b}\sum_{k=0}^{N_b-1}\eta_k\bar{\eta_k}] \\ &+ \frac{1}{2}N_b\frac{I_z}{b^2}\sum_{k=0}^{N_b-1}(\dot{\bar{\eta}_k} + i\omega\bar{\eta_k})(\dot{\eta_k} - i\omega\eta_k) \end{aligned}$$

Finally, the total kinetic energy of the helicopter writes:

$$T_p = \frac{1}{2}M\dot{z}\dot{\bar{z}} + T_{p_r}$$

with M the mass of the fuselage.

3.2 Potential energy

The potential energy of the helicopter originates from the stiffnesses of the fuselage in the two directions x and y, modeled in the figure by two springs, and

the stiffnesses of the N_b blades. The total potential energy is then the sum of the separate energies.

$$\begin{aligned} U &= \frac{1}{2}K_z z\bar{z} + \frac{1}{2}K_\beta \sum_{k=0}^{N_b-1} {\beta_k}^2 \\ &= \frac{1}{2}K_z z\bar{z} + \frac{1}{2}N_b \frac{K_\beta}{b^2} \sum_{k=0}^{N_b-1} \eta_k \bar{\eta_k} \end{aligned}$$

We assume that both of the fuselage and the rotor are isotropic, that is: $K_z = K_x = K_y$ and $K_{\beta_{k\,(k=1\cdots N_b)}} = K_\beta$.

3.3 Dissipation function

The introduction of damping to the analysis is the main contribution of this paper to the model considered by [17]. Its incorporation in the structure provides more stability to it, by absorbing the oscillation of the landing gear and reducing the lead lagging modes on the rotor: this stabilizing effect is discussed in [11] and [12] who focused only on the lag dampers.

We limit the case of study herein to linear dampers; nonlinear dampers can be replaced by equivalent linear viscous damping using a standard linearization technique [16].

Similarly to the potential energy and assuming that the rotor is isotropic, the dissipation function can be written as:

$$\begin{aligned} F &= \frac{1}{2}C_z \dot{z}\dot{\bar{z}} + \frac{1}{2}C_\beta \sum_{k=0}^{N_b-1} {\dot{\beta}_k}^2 \\ &= \frac{1}{2}C_z \dot{z}\dot{\bar{z}} + \frac{1}{2}N_b \frac{C_\beta}{b^2} \sum_{k=0}^{N_b-1} (\dot{\bar{\eta}_k} + i\omega\bar{\eta_k})(\dot{\eta_k} - i\omega\eta_k) \end{aligned}$$

Where $C_z = C_x = C_y$ and C_β is the viscous damping of each blade.

3.4 LTI model

Once we have all the energies expressions, we can write the theorem of Lagrange in order to get an LTI model of the system:

$$(\frac{\delta T}{\delta \dot{\xi}}) - (\frac{\delta T}{\delta \xi}) + (\frac{\delta U}{\delta \xi}) + (\frac{\delta F}{\delta \dot{\xi}}) = 0$$

We apply this theorem for $\xi = \bar{z}$ and $\xi = \bar{\eta_1}$. This leads to the equation of motion below:

$$\mathcal{M}_c \begin{bmatrix} \ddot{z} \\ \ddot{\eta}_1 \end{bmatrix} + \mathcal{D}_c \begin{bmatrix} \dot{z} \\ \dot{\eta}_1 \end{bmatrix} + \mathcal{K}_c \begin{bmatrix} z \\ \eta_1 \end{bmatrix} = 0$$

Where $\mathcal{M}_c$, $\mathcal{D}_c$ and $\mathcal{K}_c$ (the index c is to highlight the use of complex notation) are the mass, damping and stiffness matrices expressed as:

$$\begin{cases} \mathcal{M}_c = \begin{bmatrix} \frac{M}{N_b} + m & m \\ m & m + \frac{I_z}{b^2} \end{bmatrix} \\ \mathcal{D}_c = \begin{bmatrix} \frac{C_z}{N_b} & 0 \\ 0 & -2i\omega(m + \frac{I_z}{b^2}) + \frac{C_\beta}{b^2} \end{bmatrix} \\ \mathcal{K}_c = \begin{bmatrix} \frac{K_z}{N_b} & 0 \\ 0 & m\omega^2(\frac{a}{b} - 1 - \frac{I_z}{mb^2}) - i\omega\frac{C_\beta}{b^2} + \frac{K_\beta}{b^2} \end{bmatrix} \end{cases}$$

Let the complex state be $X_c = \begin{bmatrix} z & \eta_1 & \dot{z} & \dot{\eta_1} \end{bmatrix}^T$. We get finally the LTI system:

$$\begin{cases} \dot{X_c} = A_c X_c \\ Y_c = C_c X_c \end{cases}$$

where A_c and C_c denote the control and observation complex matrices. The vector Y_c includes the observable components of X_c. We assume that the whole state is observable:

$A_c = \begin{bmatrix} 0 & \mathcal{I} \\ -{\mathcal{M}_c}^{-1}\mathcal{K}_c & -{\mathcal{M}_c}^{-1}\mathcal{D}_c \end{bmatrix}$, $C_c = \begin{bmatrix} \mathcal{I} & 0 \end{bmatrix}$

The expressions of these matrices, in real notation: $\mathcal{M}$, $\mathcal{D}$, $\mathcal{K}$, A and C are given in appendix.

Sampling this system (in real notation) at rate $\frac{1}{\tau}$ yields the discrete time model below:

$$\begin{cases} X_{k+1} &= F\ X_k + v_{k+1} \\ Y_k &= H\ X_k + w_{k+1} \end{cases}$$

The state transition and observation matrices are: $F = e^{\tau A}$ and $H = C$. If μ is an eigenvalue of the continuous system A, the correspondent eigenvalue λ of F is such that: $\lambda = e^{\tau\mu}$.

4 Application

4.1 Modal analysis and stability

The goal of this section is to analyze the evolution of damping coefficients w.r.t the angular velocity of the rotor ω for both cases of helicopters without ($C_z = 0$ and $C_\beta = 0$) and with structural damping. Those coefficients can be computed using the eigenvalues $\lambda_{i,(i=1\cdots4)}$ of the matrix A_c such that: $\rho_i = -\frac{Re(\lambda_i)}{\sqrt{Re(\lambda_i)^2 + Im(\lambda_i)^2}}$. Therefore, a system is unstable when one or more of ρ_i are negative.

4.1.1 No damping case

In [9] and [17], it is reported that in the case where there is no damping in the rotor or in the support of the fuselage ($C_\beta = 0$ and $C_z = 0$), the neutral stability is the best we can reach. There is no evolution from a stable situation

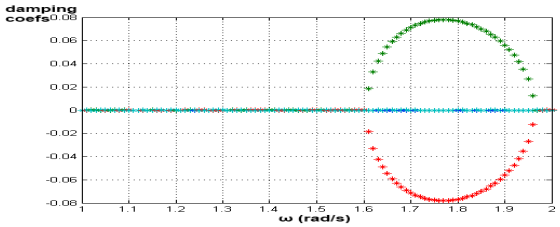

Figure 4: Modal damping coefficients vs rotation velocity in no damping case

to unstable one. Fig. 4 illustrates that indeed the modal damping coefficients are null or positive and negative at the same time.

This result was predictable; once an internal energy is created there is no damper to extract it.

4.1.2 Damping case

Fig. 5 illustrates that the damping coefficients become positive and they are varying smoothly with rotor's angular velocity. The second modal damping coefficient ρ_2 (mode 2) changes from positive values to negative ones, from $\omega \simeq 1.62\, rad.s^{-1}$ to $\omega \simeq 2\, rad.s^{-1}$, which is a criterion for ground resonance. It is this damping coefficient which will be monitored by CUSUM test.

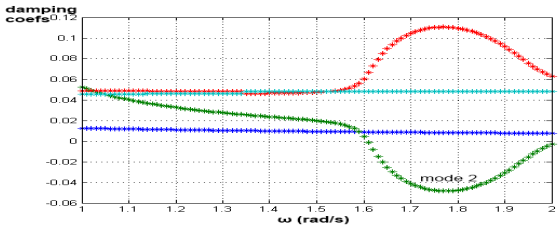

Figure 5: Modal damping coefficients vs rotation velocity in damping case

One would ask: why using the CUSUM test if we have the interval of instability from the modal analysis of the mechanical model? The answer is that this analysis is based on a deterministic method and does not take into consideration randomnesses and uncertainties (structural uncertainties, manufacturing tolerances, materials properties, erosion, airflow, loads...) that may affect the margins of stability. For instance, in [10] it is shown for the flutter phenomenon that airspeeds of instability are highly sensitive to small changes in aircraft structure. Ground resonance is similar to flutter; the use of a statistical approach will then make the detection more robust.

Remark 2 *Notice that adding a sufficient level of damping into the rotor or the support of fuselage would avoid completely the ground resonance. Unfortunately, design constraints [9] make it impossible to add large values of damping.*

4.2 Applying CUSUM test to ground resonance problem

We simulate the LTI model at rate 0.02 s, under Matlab with a gaussian white noise as an input. With complex notation, systems can not be simulated, thus we have to return to real notation (the new matrices are given in appendix). The scenario of simulation is to vary the rotation velocity ω from $1\,rad.s^{-1}$ to $2\,rad.s^{-1}$ with a step of $0.1\,rad.s^{-1}$.

We apply the CUSUM test algorithm as follows:

- compute the modal signature θ_0 at the reference: we choose $\omega = 1\,rad.s^{-1}$ as a reference
- compute the left kernel $S(\theta_0)$: we consider 10.000 samples (y_k) at the reference
- for the current modal signature corresponding to the current velocity ω, compute the estimate of the matrix of Hankel $\mathcal{H}_{p+1,q}$ from 1000 samples
- compute the estimates of the Jacobian $\mathcal{J}$ and the inverse of the matrix of covariance Σ
- start the test for the second damping coefficient ρ_2

Remark 3 *In real cases, we apply the test to every damping coefficient. But here, we have a simulation case and it is already known that ρ_2 is the only coefficient which becomes negative.*

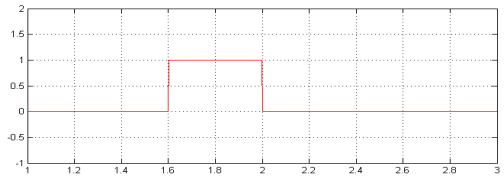

Figure 6: Response of CUSUM test: alarm vs angular velocity ω (alarm fired when $alarm = 1$)

Fig. 6 shows that the alarm is triggered at $\omega \simeq 1.6\,rad.s^{-1}$, which corresponds to the velocity of ground resonance. In fact, the test starts to respond from $\omega \simeq 1.1\,rad.s^{-1}$, but the response is significant at $\omega \simeq 1.6\,rad.s^{-1}$.

In order to obtain the other limit of instability $\omega \simeq 2\,rad.s^{-1}$, we simulate the system from $\omega = 3\,rad.s^{-1}$ to $2\,rad.s^{-1}$ with a step of $-0.1\,rad.s^{-1}$, and we apply the same algorithm with $\omega = 3\,rad.s^{-1}$ as a reference.

5 Conclusion

The problem of predicting ground resonance instability margins with off-line methods has been addressed. An on-line approach of detection using CUSUM test has been proposed and its relevance illustrated with a simulation data example.

Issues for future research encompass validation on real flight data and developing an adaptive CUSUM test with sliding reference in order to optimize the time of response of the algorithm.

References

[1] M. Basseville. On-board component fault detection and isolation using the statistical local approach. *Automatica*, 34(11):1391–1416, 1998.

[2] M. Basseville, M. Abdelghani, and A. Benveniste. Subspace-based fault detection algorithms for vibration monitoring. *Automatica*, 36:101–109, 2000.

[3] M. Basseville, A. Benveniste, M. Goursat, and L. Mevel. In-flight monitoring of aeronautic structures: vibration-based on-line automated identification versus detection. *IEEE Control Systems Magazine*, 27(5):27–42, October 2007.

[4] M. Basseville, A. Benveniste, M. Goursat, and L. Mevel. Subspace-based algorithms for structural identification, damage detection, and sensor data fusion. *Journal of Applied Signal Processing*, Special Issue on Advances in Subspace-Based Techniques for Signal Processing and Communications, 2007.

[5] M. Basseville, L. Mevel, and M. Goursat. Statistical model-based damage detection and localization: subspace-based residuals and damage-to-noise sensitivity ratios. *Journal of Sound Vibration*, 275:769–794, 2004.

[6] R. P. Coleman and A. M. Feingold. Theory of self-excited mechanical oscillations of helicopter rotors with hinged blades. Technical report, NACA, 1958.

[7] R. Donham, S. Cardinale, and I. Sachs. Ground and air resonance characteristics of a soft in-plane rigid-rotor system. *Helicopter Society*, 14(4), 1969.

[8] B. Eckert. Analytical and a numerical ground resonance analysis of a conventionally articulated main rotor helicopter. Master's thesis, Stellenbosch University, 2007.

[9] W. Johnson. *Helicopter Theory*. Dover Publications, Inc., 1994.

[10] H. H. Khodaparast, J. E. Mottershead, and K. J. Badcock. Propagation of structural uncertainty to linear aeroelastic stability. *Computers and Structures*, 88:223–236, 2010.

[11] D. L. Kunz. Influence of elastomeric damper modeling on the dynamic response of helicopter rotors. *AIAA*, 35:349–354, 1997.

[12] D. L. Kunz. Nonlinear analysis of helicopter ground resonance. *Nonlinear Analysis*, 3:383–395, 2002.

[13] L. Mevel, M. Basseville, and A. Benveniste. Fast in-flight detection of flutter onset - a statistical approach. *AIAA Jal Guidance, Control, and Dynamics*, 28(3):431–438, 2005.

[14] M. N. Nahas. Helicopter ground resonance - a spatial model analysis. *Aeronautical Journal*, 88:299–308, 1984.

[15] E. S. Page. Continuous inspection schemes. *Biometrika*, 41:100–115, 1954.

[16] L. Pang, G. M. Kamath, and N. M. Wereley. Analysis and testing of a linear stroke magnetorheological damper. In *39th AIAA/ASME/ASCE/AHS/ASC Structures, Structural Dynamics, and Materials Conference and Exhibit and AIAA/ASME/AHS Adaptive*, 1998.

[17] L. Sanches, G. Michon, A. Berlioz, and D. Alazard. Instability zones identification in multiblade rotor dynamics. In *11th Pan-American Congress of Applied Mechanics*, 2010.

[18] I. Sharf and L. Monterrubio. Influence of landing gear design on helicopter ground resonance. *AIAA*, 36:452–462, 1999.

[19] R. Zouari, L. Mevel, and M. Basseville. Cusum test for flutter monitoring of modal dynamics. In *Noise and Vibration Engineering Conference, Leuven, BE*, 2006.

A Matrices in real notation

The state vector in real notation is:

$X = \left[\begin{array}{cccccccc} x & y & Re(\eta_1) & Im(\eta_1) & \dot{x} & \dot{y} & Re(\dot{\eta_1}) & Im(\dot{\eta_1}) \end{array} \right]^T$

Then, the matrices of mass, damping and stiffness in real notation write:

$$\mathcal{M} = \left[\begin{array}{cccc} \frac{M}{N_b} + m & 0 & m & 0 \\ 0 & \frac{M}{N_b} + m & 0 & m \\ m & 0 & m + \frac{I_z}{b^2} & 0 \\ 0 & m & 0 & m + \frac{I_z}{b^2} \end{array} \right]$$

$$\mathcal{D} = \left[\begin{array}{cccc} \frac{C_z}{N_b} & 0 & 0 & 0 \\ 0 & \frac{C_z}{N_b} & 0 & 0 \\ 0 & 0 & \frac{C_\beta}{b^2} & 2\omega(m + \frac{I_z}{b^2}) \\ 0 & 0 & -2\omega(m + \frac{I_z}{b^2}) & \frac{C_\beta}{b^2} \end{array} \right]$$

$$\mathcal{K} = \left[\begin{array}{cccc} \frac{K_z}{N_b} & 0 & 0 & 0 \\ 0 & \frac{K_z}{N_b} & 0 & 0 \\ 0 & 0 & L & \omega\frac{C_\beta}{b^2} \\ 0 & 0 & -\omega\frac{C_\beta}{b^2} & L \end{array} \right]$$

where $L = m\omega^2(\frac{a}{b} - 1 - \frac{I_z}{mb^2}) + \frac{K_\beta}{b^2}$, and the matrices of transition and observation are:

$$A = \left[\begin{array}{cc} 0 & \mathcal{I} \\ -\mathcal{M}^{-1}\mathcal{K} & -\mathcal{M}^{-1}\mathcal{D} \end{array} \right], \; C = \left[\begin{array}{cc} \mathcal{I} & 0 \end{array} \right]$$

A has 8 eigenvalues but they are conjugate pairs, so we keep only 4 eigenvalues for the analysis.

Contents

Centre de recherche INRIA Rennes – Bretagne Atlantique
IRISA, Campus universitaire de Beaulieu - 35042 Rennes Cedex (France)

Centre de recherche INRIA Bordeaux – Sud Ouest : Domaine Universitaire - 351, cours de la Libération - 33405 Talence Cedex
Centre de recherche INRIA Grenoble – Rhône-Alpes : 655, avenue de l'Europe - 38334 Montbonnot Saint-Ismier
Centre de recherche INRIA Lille – Nord Europe : Parc Scientifique de la Haute Borne - 40, avenue Halley - 59650 Villeneuve d'Ascq
Centre de recherche INRIA Nancy – Grand Est : LORIA, Technopôle de Nancy-Brabois - Campus scientifique
615, rue du Jardin Botanique - BP 101 - 54602 Villers-lès-Nancy Cedex
Centre de recherche INRIA Paris – Rocquencourt : Domaine de Voluceau - Rocquencourt - BP 105 - 78153 Le Chesnay Cedex
Centre de recherche INRIA Saclay – Île-de-France : Parc Orsay Université - ZAC des Vignes : 4, rue Jacques Monod - 91893 Orsay Cedex
Centre de recherche INRIA Sophia Antipolis – Méditerranée : 2004, route des Lucioles - BP 93 - 06902 Sophia Antipolis Cedex

Éditeur
INRIA - Domaine de Voluceau - Rocquencourt, BP 105 - 78153 Le Chesnay Cedex (France)
http://www.inria.fr
ISSN 0249-6399